

Subthreshold ρ contribution in J/ψ decay to $\omega\pi\pi$ and $K\bar{K}\pi$

 F. Q. Wu^{1,2,4,*} and B. S. Zou^{1,2,3,†}
¹CCAST (World Laboratory), P. O. Box 8730, Beijing 100080, China

²Institute of High Energy Physics, CAS, Beijing 100049, China

³Institute of Theoretical Physics, CAS, Beijing 100080, China

⁴Graduate School, Chinese Academy of Sciences, Beijing 100049, China

(Received 27 March 2006; published 7 June 2006)

We carry out a theoretical and Monte Carlo study on the J/ψ decays into $\omega\pi\pi$ and $K\bar{K}\pi$ through intermediate subthreshold ρ meson by using SU(3)-symmetric Lagrangian approach. It is found that the subthreshold ρ contribution is not negligible and may have significant influence on partial wave analysis of resonances in these channels, especially near the $\omega\pi$ and $K\bar{K}$ thresholds.

DOI: 10.1103/PhysRevD.73.114008

PACS numbers: 13.25.Gv, 13.30.Eg, 13.66.Bc, 14.40.Gx

I. INTRODUCTION

In recent years, much effort has been devoted to the study of meson and baryon spectra. Of particular interests, the J/ψ decays now provide an excellent source of information for studying light hadron spectroscopy and searching for glueballs, hybrids, and exotic states [1]. Several interesting near-threshold structures were observed and studied, such as the broad σ near $\pi\pi$ threshold [2], the broad κ near $K\pi$ threshold [3], the narrow $f_0(980)$ peak near $\bar{K}K$ threshold [4], and the narrow structure near $\bar{p}p$ threshold [5]. While various mechanisms were proposed to explain these structures [6], the conventional t -channel meson exchange final state interaction mechanism [7,8] can give consistent explanation for all these structures. The t -channel ρ meson exchange was found to play a very important role for all these structures.

In this paper, we want to address two other puzzling near-threshold phenomena in J/ψ decays. The first one is the “ b_1 puzzle” in the $J/\psi \rightarrow \omega\pi\pi$. Both DM2 Collaboration [9] and BESII Collaboration [2] obtained a much broader width for the near- $\omega\pi$ -threshold resonance $b_1(1235)$: while PDG gives the width (142 ± 9) MeV [10], the DM2 and BESII gave it as (210 ± 19) MeV and (195 ± 20) MeV, respectively. The second puzzle is that there is a clear near- $\bar{K}K$ -threshold enhancement in both $J/\psi \rightarrow K^+K^-\pi^0$ and $J/\psi \rightarrow K_S K^\pm \pi^\mp$ Dalitz plots from DM2 data [11] although the structure was not addressed in the paper possibly due to uncertainty of background contribution. From conservation laws for strong interaction, the $\bar{K}K$ here should have isospin 1 and spin-parity 1^- . There is no known resonance of these quantum numbers very close to $\bar{K}K$ threshold.

It is rather tempting to claim some new near-threshold resonances here. But before claiming any new physics from the seemingly puzzling phenomena, one should investigate all possible conventional mechanisms to see if the phenomena can be interpreted within the existing theoretic

cal framework. Motivated by this idea, here we investigate the subthreshold ρ contribution to these channels through diagrams shown in Figs. 1 and 2 for $J/\psi \rightarrow \omega\pi\pi$ and $J/\psi \rightarrow \bar{K}K\pi$, respectively. There are good reasons for considering this mechanism. The $J/\psi \rightarrow \rho\pi\pi$ decay has the largest branching ratio among the known two-body decay channels of the J/ψ [10]. The ρKK and $\rho\omega\pi$ couplings are well determined to be large.

This paper is organized as follows. In Sec. II, we present the method and formulation for calculation and Monte Carlo simulation. The numerical results and discussions are given in Sec. III.

II. METHOD AND FORMULATION

The Feynman diagrams for relevant processes with the subthreshold ρ contributions are depicted in Fig. 1 ($J/\psi \rightarrow \omega\pi^+\pi^-$) and Fig. 2 ($J/\psi \rightarrow K\bar{K}\pi$). For the vector-vector-pseudoscalar (VVP) and the pseudoscalar-pseudoscalar-vector (PPV) couplings, we use the SU(3)-symmetric Lagrangians as in [8,12]

$$\mathcal{L}_{\text{VVP}} = \frac{G}{\sqrt{2}} \epsilon^{\mu\nu\alpha\beta} \langle \partial_\mu V_\nu \partial_\alpha V_\beta P \rangle, \quad (1)$$

$$\mathcal{L}_{\text{PPV}} = -\frac{1}{2} i G' \langle [P, \partial_\mu P] V^\mu \rangle, \quad (2)$$

where $\langle \dots \rangle$ means SU(3) trace, G and G' are the coupling constants, and P is the 3×3 matrix representation of the pseudoscalar meson octet, here $P = \lambda_a P^a$, $a = 1, \dots, 8$,

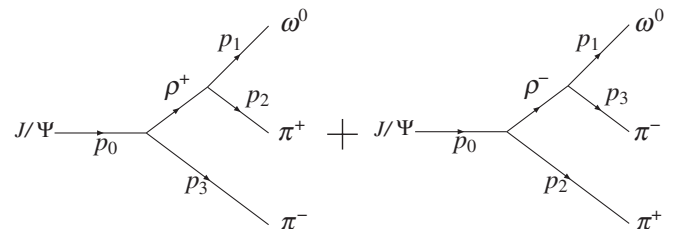


FIG. 1. Diagrams for $J/\psi \rightarrow \omega\pi^+\pi^-$ decay with subthreshold ρ exchange.

*Electronic mail: wufq@ihep.ac.cn

†Electronic mail: zoubs@ihep.ac.cn

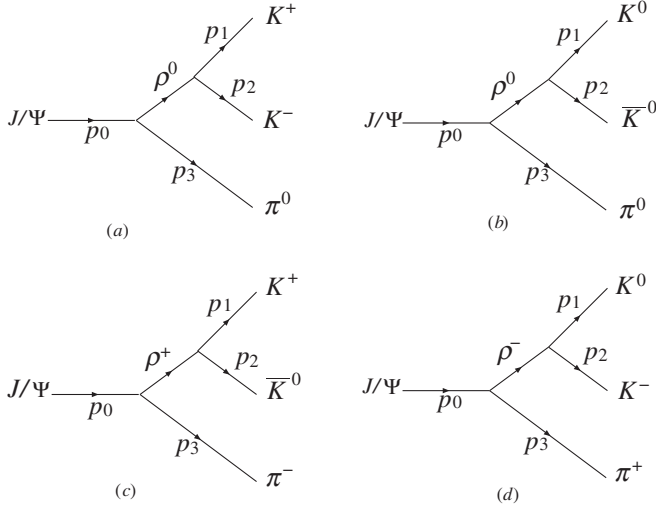


FIG. 2. Diagrams for $J/\psi \rightarrow K\bar{K}\pi$ decay with subthreshold ρ exchange.

and λ_a are the 3×3 generators of SU(3). A similar definition of V_ν is used for the vector meson octet.

In the Gell-Mann representation, the relevant effective Lagrangians are

$$\mathcal{L}_{\psi\rho\pi} = g_{\psi\rho\pi} \epsilon^{\mu\nu\alpha\beta} p_\psi^\mu e^\nu(\psi) p_\rho^\alpha e^\beta(\rho), \quad (3)$$

$$\mathcal{L}_{\omega\rho\pi} = g_{\omega\rho\pi} \epsilon^{\mu\nu\alpha\beta} p_\omega^\mu e^\nu(\omega) p_\rho^\alpha e^\beta(\rho), \quad (4)$$

$$\begin{aligned} \mathcal{L}_{\rho\pi\pi} = & g_{\rho\pi\pi} [(p_{\pi^+}^\mu - p_{\pi^-}^\mu) \rho_\mu^0 + (p_{\pi^-}^\mu - p_{\pi^0}^\mu) \rho_\mu^+ \\ & + (p_{\pi^0}^\mu - p_{\pi^+}^\mu) \rho_\mu^-], \end{aligned} \quad (5)$$

$$\begin{aligned} \mathcal{L}_{\rho K\bar{K}} = & g_{\rho K\bar{K}} [(p_{K^+}^\mu - p_{K^-}^\mu) \rho_\mu^0 + (p_{K^-}^\mu - p_{K^0}^\mu) \rho_\mu^+ \\ & + \sqrt{2} g_{\rho K\bar{K}} (p_{K^0}^\mu - p_{K^-}^\mu) \rho_\mu^+ \\ & + \sqrt{2} g_{\rho K\bar{K}} (p_{K^+}^\mu - p_{K^0}^\mu) \rho_\mu^-], \end{aligned} \quad (6)$$

where $g_{\rho K\bar{K}} = \frac{1}{2} g_{\rho\pi\pi} = G'$ due to flavor SU(3) symmetry. Using these Lagrangians, we are able to construct the following amplitudes T_1 , T_{2a} , T_{2b} , T_{2c} , and T_{2d} corresponding to the diagrams in Figs. 1 and 2(a)–2(d), respectively:

$$\begin{aligned} T_1 = & -g_{\psi\rho\pi} g_{\omega\rho\pi} \left\{ \epsilon_{\mu\nu\alpha\beta} p_0^\mu e^{*\nu}(\psi) (p_1 + p_2)^\alpha \right. \\ & \times \epsilon^{\gamma\beta\lambda\sigma} (p_1 + p_2)_\gamma p_{1\lambda} e_\sigma(\omega) \\ & \times \frac{1}{(p_1 + p_2)^2 - m_\rho^2 + im_\rho \Gamma_\rho} \\ & + \frac{1}{(p_1 + p_3)^2 - m_\rho^2 + im_\rho \Gamma_\rho} \epsilon_{\mu\nu\alpha\beta} p_0^\mu e^{*\nu}(\psi) (p_1 + p_3)^\alpha \\ & \left. \times \epsilon^{\gamma\beta\lambda\sigma} (p_1 + p_3)_\gamma p_{1\lambda} e_\sigma(\omega) \right\} F_{\psi\rho\pi} F_{\omega\rho\pi}, \end{aligned} \quad (7)$$

$$\begin{aligned} T_{2a} = T_{2b} = & \frac{1}{\sqrt{2}} T_{2c} = \frac{1}{\sqrt{2}} T_{2d} \\ = & - \frac{2g_{\psi\rho\pi} g_{\rho K\bar{K}}}{(p_1 + p_2)^2 - m_\rho^2 + im_\rho \Gamma_\rho} \\ & \times \epsilon_{\mu\nu\alpha\beta} p_0^\mu e^{*\nu}(\psi) p_1^\alpha p_2^\beta F_{\psi\rho\pi} F_{\rho K\bar{K}}. \end{aligned} \quad (8)$$

Here Γ_ρ represents the width of ρ ; $F_{\psi\rho\pi}$, $F_{\omega\rho\pi}$ and $F_{\rho K\bar{K}}$ are the form factors for the $\psi\rho\pi$, $\omega\rho\pi$, and $\rho K\bar{K}$ vertices, respectively.

Usually, hadronic form factors should be applied to the meson-meson vertices because of the inner quark-gluon structure of hadrons. It is well known that form factors play an important role in many physics processes, such as $\pi\pi$ scattering [8], NN interactions [13], πN scattering [14], meson photoproduction [15], etc. Because of the difficulties in dealing with nonperturbative QCD hadron structure, the form factors are commonly adopted phenomenologically.

The most commonly used form factors for meson-meson vertices in J/ψ decays are Blatt-Weisskopf barrier factors $B_l(Q_{abc})$ [16,17] for a decay process $a \rightarrow b + c$ with orbital angular momentum l between b and c mesons:

$$B_l(Q_{abc}, R) = \sqrt{\frac{Q_0^2}{Q_{abc}^2 + Q_0^2}} \quad \text{for } l = 1, \quad (9)$$

where

$$Q_{abc}^2 = \frac{(s_a + s_b - s_c)^2}{4s_a} - s_b \quad (10)$$

is the magnitude of \mathbf{p}_b or \mathbf{p}_c in the rest system of a ; $s_i = E_i^2 - \mathbf{p}_i^2$ with E_i and \mathbf{p}_i the energy and the tree-momentum component of p_i , respectively. Here Q_0 is a hadron ‘‘scale’’ parameter, $Q_0 = 0.197321/R$ GeV/c with R reflecting the radius of the centrifugal barrier in fm. We take $R = 0.5$ fm for $\psi\rho\pi$ vertex and $R = 0.5$ or 0.8 fm for $\omega\rho\pi$ and $\rho\pi\pi$ vertices. For the sake of convenience, we use the following shorthand notation for the $F_{\psi\rho\pi} F_{\rho mm}$ in Eqs. (7) and (8) for various channels:

$$F_1 \equiv \begin{cases} B_1(R_{\psi\rho\pi} = 0.5) B_1(R_{\rho\pi\pi} = 0.5), & J/\psi\rho \rightarrow \pi\pi\pi \\ B_1(R_{\psi\rho\pi} = 0.5) B_1(R_{\omega\rho\pi} = 0.5), & J/\psi\rho \rightarrow \omega\pi\pi, \\ B_1(R_{\psi\rho\pi} = 0.5) B_1(R_{\rho K\bar{K}} = 0.5), & J/\psi\rho \rightarrow K\bar{K}\pi \end{cases} \quad (11)$$

$$F_2 \equiv \begin{cases} B_1(R_{\psi\rho\pi} = 0.5) B_1(R_{\rho\pi\pi} = 0.8), & J/\psi\rho \rightarrow \pi\pi\pi \\ B_1(R_{\psi\rho\pi} = 0.5) B_1(R_{\omega\rho\pi} = 0.8), & J/\psi\rho \rightarrow \omega\pi\pi, \\ B_1(R_{\psi\rho\pi} = 0.5) B_1(R_{\rho K\bar{K}} = 0.8), & J/\psi\rho \rightarrow K\bar{K}\pi \end{cases} \quad (12)$$

The monopole form factor is also a frequently used s -channel form factor [8,18,19]:

$$F(\Lambda, q) = \frac{\Lambda^2 + m^2}{\Lambda^2 + q^2}, \quad (13)$$

where m and q are the mass and the four-momentum of the intermediate particle, respectively, and Λ is the so-called cutoff momentum that can be determined by fitting the experimental data. We take a commonly used value $\Lambda = 1.5$ GeV for $\rho\pi\pi$ [8] and $\omega\rho\pi$ [19] vertices. For $\rho K\bar{K}$ vertex, $\Lambda = 1.5\text{--}4.5$ GeV was used in literature [7,8]. It is possible that mesons involving heavier quarks have smaller size and the corresponding need larger cutoff Λ parameter for the relevant vertices. We take $\Lambda = 1.5\text{--}4.5$ GeV for $J/\psi\rho\pi$ vertex and $\rho K\bar{K}$ vertex. Similarly, we define

$$F_3 \equiv \begin{cases} F(\Lambda_{\psi\rho\pi} = 4.5)F(\Lambda_{\rho\pi\pi} = 1.5), & J/\psi\rho \rightarrow \pi\pi\pi \\ F(\Lambda_{\psi\rho\pi} = 4.5)F(\Lambda_{\omega\rho\pi} = 1.5), & J/\psi\rho \rightarrow \omega\pi\pi, \\ F(\Lambda_{\psi\rho\pi} = 4.5)F(\Lambda_{\rho K\bar{K}} = 1.5 - 4.5), & J/\psi\rho \rightarrow K\bar{K}\pi \end{cases} \quad (14)$$

$$F_4 \equiv \begin{cases} F(\Lambda_{\psi\rho\pi} = 1.5)F(\Lambda_{\rho\pi\pi} = 1.5), & J/\psi\rho \rightarrow \pi\pi\pi \\ F(\Lambda_{\psi\rho\pi} = 1.5)F(\Lambda_{\omega\rho\pi} = 1.5), & J/\psi\rho \rightarrow \omega\pi\pi, \\ F(\Lambda_{\psi\rho\pi} = 1.5)F(\Lambda_{\rho K\bar{K}} = 1.5 - 4.5), & J/\psi\rho \rightarrow K\bar{K}\pi \end{cases} \quad (15)$$

The differential decay widths can be evaluated as

$$d\Gamma(J/\psi \rightarrow \omega\pi^+\pi^-) = \frac{(2\pi)^4}{2M_\psi} |T_1|^2 d\Phi_3(p_0; p_1, p_2, p_3), \quad (16)$$

$$d\Gamma(J/\psi \rightarrow K\bar{K}\pi) = \frac{(2\pi)^4}{2M_\psi} (|T_{2a}|^2 + |T_{2b}|^2 + |T_{2c}|^2 + |T_{2d}|^2) d\Phi_3(p_0; p_1, p_2, p_3), \quad (17)$$

with M_ψ being the mass of J/ψ and the three-body phase space factor

$$d\Phi_3(p_0; p_1, p_2, p_3) = \delta^4(p_0 - p_1 - p_2 - p_3) \frac{d^3 p_1}{(2\pi)^3 2E_1} \times \frac{d^3 p_2}{(2\pi)^3 2E_2} \frac{d^3 p_3}{(2\pi)^3 2E_3}. \quad (18)$$

From the above equations and following the covariant tensor amplitude method described in detail in Refs. [17], the entire calculations are straightforward although tedious. The numerical results are given in the following section.

III. NUMERICAL RESULTS AND DISCUSSIONS

In the model described so far, there are four relevant coupling constants, $g_{\psi\rho\pi}$, $g_{\omega\rho\pi}$, and $g_{\rho\pi\pi}$ (see Eqs. (3)–(6)). The $g_{\rho\pi\pi}$ can be obtained by evaluating the process $\rho \rightarrow \pi\pi$ with various form factors. In an analogous way, we can obtain $g_{\psi\rho\pi}$ through the sequential decays $\psi \rightarrow \rho\pi$ with $\rho \rightarrow \pi\pi$ and $g_{\omega\rho\pi}$ through $\omega \rightarrow \rho\pi$ with $\rho \rightarrow \pi\pi$

by using the similar approach described in the section above. The experimental data of $\rho \rightarrow \pi\pi$, $\psi \rightarrow \rho\pi$, $\omega \rightarrow \pi\pi\pi$ decay widths are from the PDG [10]. The results are shown in Table I.

We use two forms of Γ_ρ in Eqs. (7) and (8). First we take it as a constant of 0.149 GeV. Then we take an energy dependent width including $\pi\pi$, $\omega\pi$, and $K\bar{K}$ channels

$$\Gamma_\rho(s) = \Gamma_{\rho \rightarrow \pi\pi}(s) + \Gamma_{\rho \rightarrow \omega\pi}(s) + \Gamma_{\rho \rightarrow K\bar{K}}(s) \equiv \Gamma_{\rho \rightarrow (\pi\pi + \omega\pi + K\bar{K})}, \quad (19)$$

where energy dependent partial width $\Gamma_{\rho \rightarrow \pi\pi}$, $\Gamma_{\rho \rightarrow \omega\pi}$, and $\Gamma_{\rho \rightarrow K\bar{K}}$ are obtained by the method similar to Eqs. (16) and (17). Usually only $\rho \rightarrow \pi\pi$ width is considered in the ρ propagator. But in reality, when the invariant mass of the off-peak ρ meson goes above $\omega\pi$ and $K\bar{K}$ thresholds, the off-peak ρ can also decay into these new channels and the corresponding partial decay widths should be included in its total energy dependent width. This will make the tail of ρ propagator drop faster for energies above the new thresholds than the usual propagator with constant width. We find that the two forms of Γ_ρ have little influence on coupling constants. So we use the same coupling constants in amplitudes with the same form factor (see Table I).

In order to demonstrate how large effect the s -channel subthreshold ρ exchange may have upon various channels, their contributions are calculated and compared with experimental decay widths of the corresponding final states. The results are listed in Table I. The $R_{\omega\pi\pi}^\rho$ and $R_{K\bar{K}\pi}^\rho$ represent the ratio of theoretical contribution from the subthreshold ρ exchange to the experimental width taken from PDG [10] for the channels $\omega\pi^+\pi^-$ and $K\bar{K}\pi$, respectively:

$$R_{\omega\pi\pi}^\rho \equiv \frac{\Gamma_{th}(J/\psi \rightarrow \rho \omega \pi^+ \pi^-)}{\Gamma_{ex}(J/\psi \rightarrow \omega \pi^+ \pi^-)}, \quad (20)$$

$$R_{K\bar{K}\pi}^\rho \equiv \frac{\Gamma_{th}(J/\psi \rightarrow \rho K\bar{K}\pi)}{\Gamma_{ex}(J/\psi \rightarrow K\bar{K}\pi)}. \quad (21)$$

The range of variations for $R_{K\bar{K}\pi}^\rho$ in Table I for form factor F_3 and F_4 comes from the variation of Λ between 1.5 and 4.5 GeV for the $\rho K\bar{K}$ vertex.

From Table I, we see that no matter which form of Γ_ρ and form factor are employed, the range of the $R_{\omega\pi\pi}^\rho$ is from 3.1% to 21.0% and that of $R_{K\bar{K}\pi}^\rho$ is from 0.9% to 4.5%. It means that the contribution of the s -channel subthreshold ρ exchange is not negligible for both $J/\psi \rightarrow \omega\pi\pi$ and $J/\psi \rightarrow K\bar{K}\pi$ channels. The subthreshold ρ contribution may have significant influence on the analysis of resonances near $\omega\pi$ and $K\bar{K}$ thresholds.

In order to see the influence it may have on the analysis of resonances near thresholds, we perform a Monte Carlo simulation to give predictions on various invariant-mass spectra and Dalitz plots for these two channels as shown in

TABLE I. The coupling constants and the percentages of the s -channel subthreshold ρ exchange contribution as functions of the form factors (F. F.) and of the choice of ρ width.

F. F.	Γ_ρ (GeV)	$g_{\rho\pi\pi}$	$g_{J/\psi\rho\pi}$ (GeV^{-1})	$g_{\omega\rho\pi}$ (GeV^{-1})	$R_{\omega\pi\pi}^\rho$ (%)	$R_{K\bar{K}\pi}^\rho$ (%)
F_1	0.149	8.18	8.61	14.56	21.0	4.5
	$\Gamma_{\rho \rightarrow (\pi\pi + \omega\pi + K\bar{K})}$		$\times 10^{-3}$		18.3	4.3
F_2	0.149	10.69	8.70	14.68	11.1	4.2
	$\Gamma_{\rho \rightarrow (\pi\pi + \omega\pi + K\bar{K})}$		$\times 10^{-3}$		9.3	4.0
F_3	0.149	6.05	2.31	11.82	7.7	1.7–3.4
	$\Gamma_{\rho \rightarrow (\pi\pi + \omega\pi + K\bar{K})}$		$\times 10^{-3}$		6.3	1.6–3.2
F_4	0.149	6.05	2.35	11.82	3.9	1.0–1.8
	$\Gamma_{\rho \rightarrow (\pi\pi + \omega\pi + K\bar{K})}$		$\times 10^{-3}$		3.1	0.9–1.7

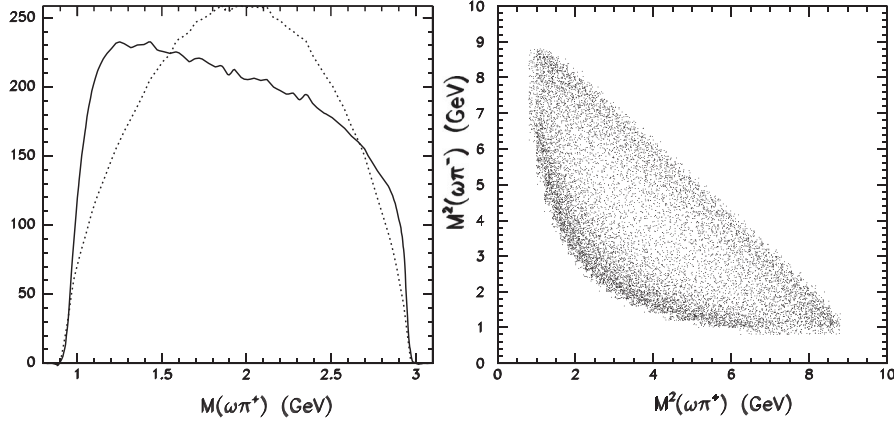


FIG. 3. The $\omega\pi$ invariant-mass distribution (solid line) and the Dalitz plot for $J/\psi \rightarrow \omega\pi^+\pi^-$ decay through ρ exchange with form factor F_2 and $\Gamma_\rho = 0.149$ GeV, compared with phase space distribution (dotted line).

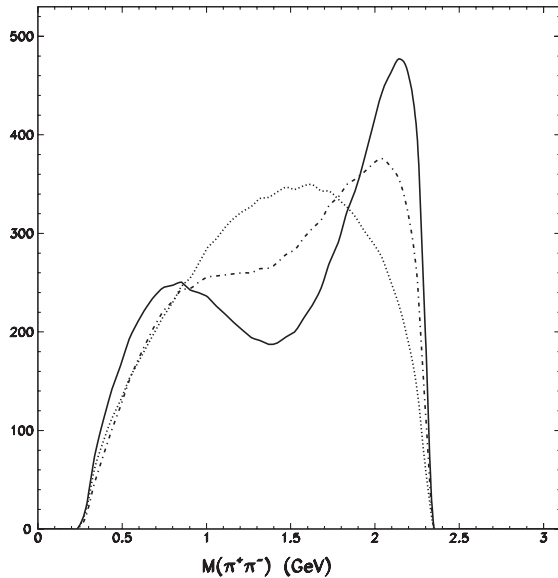


FIG. 4. The $\pi\pi$ invariant-mass distribution for $J/\psi \rightarrow \omega\pi^+\pi^-$ decay through ρ exchange with form factor F_2 and $\Gamma_\rho = 0.149$ GeV (solid line), compared with the phase space distribution (dotted line) and the result ignoring the interference effect between subthreshold ρ^+ and ρ^- contributions (dot-dashed line).

Figs. 3–5, in which we take form factor F_2 and $\Gamma_\rho = 0.149$ GeV. The dotted lines in the invariant-mass spectra denote the uniform phase space distributions without considering the dynamical interactions. In Fig. 3, a clear enhancement about 1.2 GeV near the $\omega\pi$ threshold appears in both invariant-mass spectrum and Dalitz plot. Comparing with experimental results (Fig. 7 and Fig. 10 in Ref. [9]; Fig. 1 and Fig. 2 in Ref. [2]), one can expect that this enhancement, as the background of $b_1(1235)$, should reduce the measured width of $b_1(1235)$ from this reaction and may well explain the “ b_1 puzzle.”

One interesting phenomena in the Dalitz plot of Fig. 3 is that there is also a clear enhancement band near $\pi\pi$ threshold, which is shown more clearly in the Fig. 4 for the $\pi\pi$ invariant-mass distribution of $J/\psi \rightarrow \omega\pi^+\pi^-$ decay (solid line). This enhancement band comes mainly from the interference terms of two Feynman diagrams in Fig. 1, because if we do not include the interference term of Fig. 1, the visible bump located in 0.5–1.0 GeV will be much reduced in the $\pi^+\pi^-$ invariant-mass distribution as shown by the dot-dashed line. Therefore, the subthreshold ρ contribution may even have influence upon the analysis of the σ meson from this channel.

In Fig. 5, a clear peak around 1.1 GeV near the threshold is also seen in the $K\bar{K}$ invariant-mass distribution. By

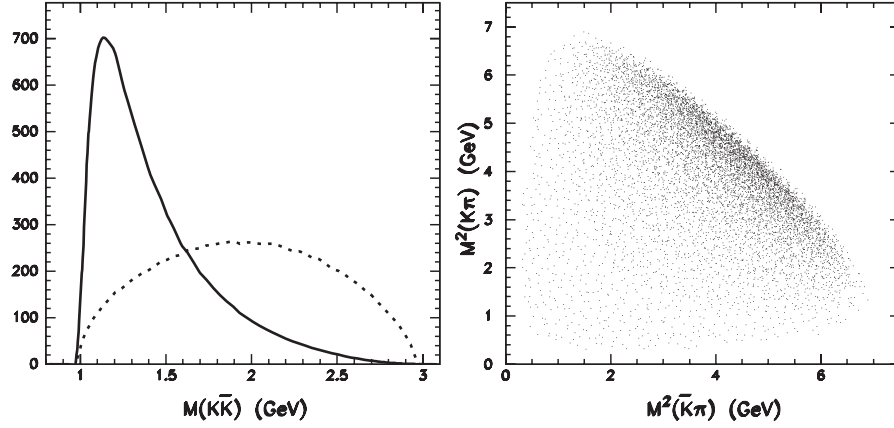


FIG. 5. The $K\bar{K}$ invariant-mass distribution (solid line) and the Dalitz plot for $J/\psi \rightarrow K\bar{K}\pi$ decay through ρ exchange with form factor F_2 and $\Gamma_\rho = 0.149$ GeV, compared with phase space distribution (dotted line).

looking at Table I and Fig. 5, it is natural to expect that the subthreshold ρ contribution is an important source for the near-threshold enhancement found in $J/\psi \rightarrow K^+K^-\pi^0$ decay by the DM2 Collaboration [11]. Hence the result provides another evidence of the important role played by the subthreshold ρ contribution.

Since the mass of ρ is more than 150 MeV below the $\omega\pi$ and $K\bar{K}$ thresholds and the width of ρ is not very broad, some people naively assume that the subthreshold ρ contribution can be neglected in these channels of J/ψ decays. However, this paper should greatly change this point of view for the channels with final state particles coupling strongly to the subthreshold ρ . A similar important subthreshold contribution was previously noticed for $J/\psi \rightarrow \bar{N}N\pi$ channels from the subthreshold nucleon pole [20].

In summary, the ρ exchange plays a very important role in many low-energy strong interaction processes, such as $\pi\pi$ scattering, πK scattering, πN interaction, etc. In this paper, we extend the mechanism to interpret some long-

standing problems observed in J/ψ decays. It is found that the subthreshold ρ contribution is not negligible for both $J/\psi \rightarrow \omega\pi\pi$ and $J/\psi \rightarrow K\bar{K}\pi$ channels, and should be included in analyzing these channels. It may well explain the long-standing b_1 puzzle near the $\omega\pi$ threshold in $J/\psi \rightarrow \omega\pi\pi$ and the near $K\bar{K}$ threshold enhancement in $J/\psi \rightarrow K\bar{K}\pi$ decay.

ACKNOWLEDGMENTS

We acknowledge stimulating discussions with BES members on relevant issues. One of us (Wu) would like to thank Bo-Chao Liu, Ju-Jun Xie, Xin Zhang, Feng-Kun Guo, and Hai-Qing Zhou for valuable comments and discussions during the preparation of this paper. This work is partly supported by the National Nature Science Foundation of China under Grants No. 10225525, No. 10435080, and by the Chinese Academy of Sciences under Project No. KJCX2-SW-N02.

-
- [1] W. Li (BES Collaboration), *Int. J. Mod. Phys. A* **20**, 1560 (2005); X. Shen (BES Collaboration), *Int. J. Mod. Phys. A* **20**, 1706 (2005); B. S. Zou, *Nucl. Phys. A* **692**, 362 (2001); C. Z. Yuan, *AIP Conf. Proc. No. 814* (AIP, New York, 2006), p. 65; B. C. Liu and B. S. Zou, *Phys. Rev. Lett.* **96**, 042002 (2006).
- [2] M. Ablikim *et al.* (BES Collaboration), *Phys. Lett. B* **598**, 149 (2004).
- [3] M. Ablikim *et al.* (BES Collaboration), *Phys. Lett. B* **633**, 681 (2006).
- [4] M. Ablikim *et al.* (BES Collaboration), *Phys. Rev. D* **70**, 092002 (2004).
- [5] J. Z. Bai *et al.* (BES Collaboration), *Phys. Rev. Lett.* **91**, 022001 (2003).
- [6] H. Q. Zheng, Z. Y. Zhou, G. Y. Qin, Z. G. Xiao, J. J. Wang, and N. Wu, *Nucl. Phys. A* **733**, 235 (2004); D. V. Bugg, *Phys. Lett. B* **598**, 8 (2004); B. Kerbikov, A. Stavinsky, and V. Fedotov, *Phys. Rev. C* **69**, 055205 (2004); M. L. Yan, Si Li, Bin Wu, and B. Q. Ma, *Phys. Rev. D* **72**, 034027 (2005); T. D. Cohen, B. A. Gelman, and S. Nussinov, *Phys. Lett. B* **578**, 359 (2004).
- [7] D. Lohse, J. W. Durso, K. Holinde, and J. Speth, *Nucl. Phys. A* **516**, 513 (1990); S. Krewald, R. H. Lemmer, and F. P. Sassen, *Phys. Rev. D* **69**, 016003 (2004); B. S. Zou and D. V. Bugg, *Phys. Rev. D* **50**, 591 (1994); B. S. Zou and H. C. Chiang, *Phys. Rev. D* **69**, 034004 (2004); A. Sibirtsev, J. Haidenbauer, S. Krewald, Ulf-G. Meissner, and A. W. Thomas, *Phys. Rev. D* **71**, 054010 (2005).

- [8] F. Q. Wu and B. S. Zou, *Int. J. Mod. Phys. A* **20**, 1905 (2005); F. Q. Wu, B. S. Zou, L. Li, and D. V. Bugg, *Nucl. Phys. A* **735**, 111 (2004); L. Li, B. S. Zou, and G. L. Li, *Phys. Rev. D* **67**, 034025 (2003).
- [9] J. E. Augustin *et al.* (DM2 Collaboration), *Nucl. Phys. B* **320**, 1 (1989).
- [10] S. Eidelman *et al.* (Particle Data Group), *Phys. Lett. B* **592**, 1 (2004).
- [11] J. Jousset *et al.* (DM2 Collaboration), *Phys. Rev. D* **41**, 1389 (1990).
- [12] A. Bramon, R. Escribano, J. L. Lucio, and M. Napsuciale, *Phys. Lett. B* **517**, 345 (2001); L. Roca, J. E. Palomar, E. Oset, and H. C. Chiang, *Nucl. Phys. A* **744**, 127 (2004); F. Klingl, N. Kaiser, and W. Weise, *Z. Phys. A* **356**, 193 (1996).
- [13] R. Machleidt, K. Holinde, and Ch. Elster, *Phys. Rep.* **149**, 1 (1987); F. Gross, J. W. Van Orden, and K. Holinde, *Phys. Rev. C* **45**, 2094 (1992).
- [14] B. C. Pearce and B. K. Jennings, *Nucl. Phys. A* **528**, 655 (1991); C. Schütz, J. W. Durso, K. Holinde, and J. Speth, *Phys. Rev. C* **49**, 2671 (1994).
- [15] Q. Zhao, Z. Li, and C. Bennhold, *Phys. Rev. C* **58**, 2393 (1998); Q. Zhao, B. Saghai, and J. S. Al-Khalili, *Phys. Lett. B* **509**, 231 (2001); T. Sato and T.-S. H. Lee, *Phys. Rev. C* **54**, 2660 (1996).
- [16] F. Von Hippel and C. Quigg, *Phys. Rev. D* **5**, 624 (1972).
- [17] S. U. Chung, *Phys. Rev. D* **48**, 1225 (1993); B. S. Zou and D. V. Bugg, *Eur. Phys. J. A* **16**, 537 (2003).
- [18] L. C. Liu and W. X. Ma, *J. Phys. G* **26**, L59 (2000).
- [19] A. I. Titov, B. Kampfer, and B. L. Reznik, *Phys. Rev. C* **65**, 065202 (2002); A. Sibirtsev and W. Cassing, *Eur. Phys. J. A* **7**, 407 (2000); Y. Oh and T. S. H. Lee, *Phys. Rev. C* **66**, 045201 (2002).
- [20] R. Sinha and S. Okubo, *Phys. Rev. D* **30**, 2333 (1984); W.-H. Liang, P.-N. Shen, B. S. Zou, and A. Faessler, *Eur. Phys. J. A* **21**, 487 (2004).